Modeling a Fixed-Wing UAV

A Collection of Equations

George Zogopoulos - Papaliakos

NATIONAL TECHNICAL UNIVERSITY OF ATHENS

SCHOOL OF MECHANICAL ENGINEERING
CONTROL SYSTEMS LABORATORY

e-mail: gzogop@mail.ntua.gr

Athens , July 13, 2016

Document version: 2.0

Todo list

Contents

Revision History

Revision	Date	Author(s)	Description
1.0	2015-01-21	GZP	Release
1.1	2015-01-22	GZP	Fixed broken references, Fixed error in eq 5.1 and expanded it, Corrected definition of rotation matrix, Added cross product matrix expansion
1.2	2015-01-23	GZP	Corrected eq 5.7
1.3	2015-01-23	GZP	Un-emphasized eq 3.3 components, Fixed typo in eq 4.23
1.4	2016-07-08	GZP	Introduced code snippets to accompany equations
2.0	2016-07-11	GZP	Separated the external environment models to a new chapter, Created multiple sub-files, Typo fixes, Notation fixes, Added some figures, Added Beard engine model

Chapter 1

Introduction for the Second Version

This document is the answer to my need to have all my aircraft equations and UAV-related models in one place, with reliable literature to support them. I has already been useful to me as a reference and as a quick source of models for my colleagues, and I hope you will find it equally useful.

The second version of this document signals two significant changes.

First of all, I have decided to include C-style code snippets for all derivations. When using models containing vector operations or dynamic equations, their implementation often presents difficulties and a lot of head-scratching. Converting the multiplication of a rotation matrix with a vector, for use in an embedded computer is a sore example; one simple equation can take forever to write. By having the code-snippets readily available I hope to help anyone who undertakes a simulation project from the beginning have a head-start (including me).

Also, the document will no longer be placed under the umbrella of the Basic Air Data project (`www.basicairdata.eu`), since I, myself, am no longer part of it. I now develop it during my work as a PhD candidate and the university logo sits at the front page.

Chapter 2

Kinematic Equations

Considering the UAV as a rigid body, the standard kinematic equations can be used. Due to the scope of this analysis, the **Flat-Earth model** equations will be used, instead of a round Earth (eg WGS-84 model). This option was made since the intended UAV area of operations will be constrained over a small area. GPS coordinates will be used as in a Cartesian grid.

2.1   Position

We express the position vector as

$$\boldsymbol{p} = [n \ e \ d]^T \tag{2.1}$$

The variables n, e and d correspond to the North, East and Down direction, which constitute the primary axis of the NED (as it is called) coordinate system. We shall denote this frame as $\mathcal{F}_F$. The origin of the NED frame is arbitrarily located at the home of operations (or launch point) of every mission and placed on the surface of the Earth. In contrast, the origin of the so-called body-axes $\mathcal{F}_B$ is the center of gravity point of the aircraft. Its x-axis is placed on the line of longitudinal symmetry, its y-axis starboard and the z-axis downwards, producing a right-handed frame, which can be seen in the following figure.
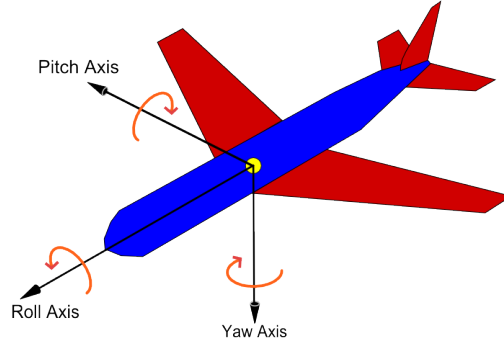
Figure 2.1: Aircraft body axes

The derivative of the position is

$$\dot{\boldsymbol{p}} = \boldsymbol{R}_b^T \boldsymbol{v_b} \tag{2.2}$$

We denote with R_b the transformation matrix **from the Inertial frame to the Body frame**. Its elements are:

$$\boldsymbol{R}_b = \begin{bmatrix} \cos\theta\cos\psi & \cos\theta\sin\psi & -\sin\theta \\ -\cos\phi\sin\psi + \sin\phi\sin\theta\cos\psi & \cos\phi\cos\psi + \sin\phi\sin\theta\sin\psi & \sin\phi\cos\theta \\ \sin\phi\sin\psi + \cos\phi\sin\theta\cos\psi & -\sin\phi\cos\psi + \cos\phi\sin\theta\sin\psi & \cos\phi\cos\theta \end{bmatrix} \tag{2.3}$$

Equation (2.2) can be broken down onto its three elements as

$$\dot{n} = (\cos\theta\cos\psi)u + (-\cos\phi\sin\psi + \sin\phi\sin\theta\cos\psi)v$$
$$+ (\sin\phi\sin\psi + \cos\phi\sin\theta\cos\psi)w \tag{2.3a}$$
$$\dot{e} = (\cos\theta\sin\psi)u + (\cos\phi\cos\psi + \sin\phi\sin\theta\sin\psi)v$$
$$+ (-\sin\phi\cos\psi + \cos\phi\sin\theta\sin\psi)w \tag{2.3b}$$
$$\dot{d} = (-\sin\theta)u + (\sin\phi\cos\theta)v + (\cos\phi\cos\theta)w \tag{2.3c}$$

```
dot_north = (cos(theta)*cos(psi))*u + (-cos(phi)*sin(psi)+sin(phi)*
    sin(theta)*cos(psi))*v + (sin(phi)*sin(psi)+cos(phi)*sin(theta)
    *cos(psi))*w
dot_east = (cos(theta)*sin(psi))*u + (cos(phi)*cos(psi)+sin(phi)*
    sin(theta)*sin(psi))*v + (-sin(phi)*cos(psi)+cos(phi)*sin(theta
    )*sin(psi))*w
dot_down = (-sin(theta))*u + (sin(phi)*cos(theta))*v + (cos(phi)*
    cos(theta))*w
```

We see that the rotation matrix $\boldsymbol{R_b}$ is dependent upon three variables, ϕ, θ and ψ. These are explained below.

In case the linear velocities need to be extracted from the position derivatives, the inverse relation can be used.

$$u = (\cos\theta\cos\psi)\dot{n} + (\cos\theta\sin\psi)\dot{e} + (-\sin\theta)\dot{d} \tag{2.4a}$$

$$v = (\sin\phi\sin\theta\cos\psi - \cos\phi\sin\psi)\dot{n}$$
$$+ (\sin\phi\sin\theta\sin\psi + \cos\phi\cos\psi)\dot{e} + (\sin\phi\cos\theta)\dot{d} \tag{2.4b}$$

$$w = (\cos\phi\sin\theta\cos\psi + \sin\phi\sin\psi)\dot{n}$$
$$(\cos\phi\sin\theta\sin\psi - \sin\phi\cos\psi)\dot{e} + (\cos\phi\cos\theta)\dot{d} \tag{2.4c}$$

```
u = (cos(theta)*cos(psi))*dot_n + (cos(theta)*sin(psi))*dot_e + (-
   sin(theta))*dot_n
v = (sin(phi)*sin(theta)*cos(psi)-cos(phi)*sin(psi))*dot_n + (sin(
   phi)*sin(theta)*sin(psi)+cos(phi)*cos(psi))*dot_e + (sin(phi)*
   cos(theta))*dot_d
w = (cos(phi)*sin(theta)*cos(psi)+sin(phi)*sin(psi))*dot_n + (cos(
   phi)*sin(theta)*sin(psi)-sin(phi)*cos(psi))*dot_e + (cos(phi)*
   cos(theta))*dot_d
```

2.2   Orientation

We use Euler angle notation to express the orientation of the aircraft. Roll, pitch and yaw are denoted as ϕ, θ and ψ respectively.

$$\boldsymbol{\Phi} = [\phi\ \theta\ \psi]^T \tag{2.5}$$

Figure 2.2 has a visual representation of those angles. Take a note at the order of rotations: the standard order for aircraft applications, in order to come up with the body frame $\mathcal{F}_B$, starting from the NED frame is:

1. Rotate around NED z-axis by angle ψ, producing frame $\mathcal{F}_1$

2. Rotate around $\mathcal{F}_1$ y-axis by angle θ, producing frame $\mathcal{F}_2$

3. Rotate around $\mathcal{F}_2$ x-axis by angle ϕ, producing the $\mathcal{F}_B$ frame
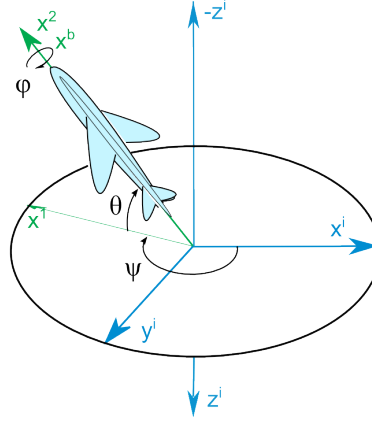
This convention is called the *Tait-Bryan angles* [6]

Figure 2.2: Euler angles

The time derivative of the Euler angles is

$$\dot{\boldsymbol{\Phi}} = \mathcal{E}(\boldsymbol{\Phi})\boldsymbol{\omega_b} \qquad (2.6)$$

where $\mathcal{E}(\boldsymbol{\Phi})$ is a rotation matrix, dependent upon the current orientation.

The individual angle propagation equations are

$$\dot{\phi} = p + \tan\theta\sin\phi q + \tan\theta\cos\phi r \qquad (2.6a)$$
$$\dot{\theta} = \cos\phi q - \sin\phi r \qquad (2.6b)$$
$$\dot{\psi} = \frac{\sin\phi}{\cos\theta}q + \frac{\cos\phi}{\cos\theta}r \qquad (2.6c)$$

```
dot_phi = p + (tan(theta)*sin(phi))*q + (tan(theta)*cos(phi))*r
dot_theta = (cos(phi))*q + (-sin(phi))*r
dot_psi = (sin(phi)/cos(theta))*q + (cos(phi)/cos(theta))*r
```

and equivalenty, $\mathcal{E}(\boldsymbol{\Phi})$ is written as

$$\mathcal{E}(\boldsymbol{\Phi}) = \begin{bmatrix} 1 & \tan\theta\sin\phi & \tan\theta\cos\phi \\ 0 & \cos\phi & -\sin\phi \\ 0 & \frac{\sin\phi}{\cos\theta} & \frac{\cos\phi}{\cos\theta} \end{bmatrix} \qquad (2.7)$$

2.3 Angular velocity

We define the angular velocity vector as

$$\boldsymbol{\omega} = [p\ q\ r]^T \qquad (2.8)$$

and its time derivative is

$$\dot{\boldsymbol{\omega}} = \frac{1}{\boldsymbol{J}}\left(\boldsymbol{T_b} - \boldsymbol{\omega} \times (\boldsymbol{J}\boldsymbol{\omega})\right) \qquad (2.9)$$

This equation incorporates the inertia matrix $\boldsymbol{J}$ and the input torque, expressed in the body axes $\boldsymbol{T_b}$.

The inertia matrix is defined as

$$\boldsymbol{J} = \begin{bmatrix} \int(y^2 + z^2)\,dm & -\int xy\,dm & -\int xz\,dm \\ -\int xy\,dm & \int(x^2 + z^2)\,dm & -\int yz\,dm \\ -\int xz\,dm & -\int yz\,dm & \int(x^2 + y^2)\,dm \end{bmatrix} \tag{2.10}$$

Commonly, the inertia matrix in fixed-wing aircraft is considered to have zero elements in the x-y and y-z direction, since they are symmetric about the x-z plane. Still, in this section, the full, non-symmetric matrix of inertia will be used, as this is the most general case.

$$\boldsymbol{J} = \begin{bmatrix} J_x & 0 & -J_{xz} \\ 0 & J_y & 0 \\ -J_{xz} & 0 & J_z \end{bmatrix} \tag{2.11}$$

Its inverse is

$$\boldsymbol{J}^{-1} = \frac{1}{det(\boldsymbol{J})} \begin{bmatrix} j_{yy}\,j_{zz} - j_{yz}\,j_{zy} & j_{xz}\,j_{zy} - j_{xy}\,j_{zz} & j_{xy}\,j_{yz} - j_{xz}\,j_{yy} \\ j_{yz}\,j_{zx} - j_{yx}\,j_{zz} & j_{xx}\,j_{zz} - j_{xz}\,j_{zx} & j_{xz}\,j_{yx} - j_{xx}\,j_{yz} \\ j_{yx}\,j_{zy} - j_{yy}\,j_{zx} & j_{xy}\,j_{zx} - j_{xx}\,j_{zy} & j_{xx}\,j_{yy} - j_{xy}\,j_{yx} \end{bmatrix} \tag{2.12}$$

```
Ji[0] = (J[4]*J[8] - J[5]*J[7])/detJ
Ji[1] = (J[2]*J[7] - J[1]*J[8])/detJ
Ji[2] = (J[1]*J[5] - J[2]*J[4])/detJ
Ji[3] = (J[5]*J[6] - J[3]*J[8])/detJ
Ji[4] = (J[0]*J[8] - J[2]*J[6])/detJ
Ji[5] = (J[2]*J[3] - J[0]*J[5])/detJ
Ji[6] = (J[3]*J[7] - J[4]*J[6])/detJ
Ji[7] = (J[1]*J[6] - J[0]*J[7])/detJ
Ji[8] = (J[0]*J[4] - J[1]*J[3])/detJ
```

where

$$det(\boldsymbol{J}) = j_{xx}\,j_{yy}\,j_{zz} - j_{xx}\,j_{yz}\,j_{zy} - j_{xy}\,j_{yx}\,j_{zz} + j_{xy}\,j_{yz}\,j_{zx} + j_{xz}\,j_{yx}\,j_{zy} - j_{xz}\,j_{yy}\,j_{zx} \tag{2.13}$$

```
detJ = J[0]*J[4]*J8] - J[0]*J[5]*J[7] - J[1]*J[3]*J[8] + J[1]*J[5]*
    J[6] + J[2]*J[3]*J[7] - J[2]*J[4]*J[6]
```

Cross products can be written in matrix form, when implemented as explicit matrix multiplications:

$$\boldsymbol{\omega} \times \boldsymbol{v} = \begin{bmatrix} 0 & -r & p \\ r & 0 & -p \\ -q & p & 0 \end{bmatrix} \boldsymbol{v} \tag{2.14}$$

Where $\boldsymbol{v}$ is an arbitrary vector. Similarly,

$$\boldsymbol{\omega} \times (\boldsymbol{\omega} \times \boldsymbol{v}) = \begin{bmatrix} -r^2 - q^2 & pq & pr \\ pq & -p^2 - r^2 & qr \\ pr & qr & -p^2 - q^2 \end{bmatrix} \boldsymbol{v} \qquad (2.15)$$

To facilitate derivations, we define

$$\boldsymbol{C} = \boldsymbol{\omega} \times (\boldsymbol{J}\boldsymbol{\omega}) \qquad (2.16)$$

$$= \begin{bmatrix} 0 & -r & q \\ r & 0 & -p \\ -q & p & 0 \end{bmatrix} \left(\begin{bmatrix} j_{xx} + j_{xy} + j_{xz} \\ j_{yx} + j_{yy} + j_{yz} \\ j_{zx} + j_{zy} + j_{zz} \end{bmatrix} \begin{bmatrix} p \\ q \\ r \end{bmatrix} \right) \qquad (2.17)$$

$$= \begin{bmatrix} q\left(j_{zx}p + j_{zy}q + j_{zz}r\right) - r\left(j_{yx}p + j_{yy}q + j_{yz}r\right) \\ r\left(j_{xx}p + j_{xy}q + j_{xz}r\right) - p\left(j_{zx}p + j_{zy}q + j_{zz}r\right) \\ p\left(j_{yx}p + j_{yy}q + j_{yz}r\right) - q\left(j_{xx}p + j_{xy}q + j_{xz}r\right) \end{bmatrix} \qquad (2.18)$$

```
C[0] = q*(J[6]*p + J[7]*q + J[8]*r) - r*(J[3]*p + J[4]*q + J[5]*r)
C[1] = r*(J[0]*p + J[1]*q + J[2]*r) - p*(J[6]*p + J[7]*q + J[8]*r)
C[2] = p*(J[3]*p + J[4]*q + J[5]*r) - q*(J[0]*p + J[1]*q + J[2]*r)
```

and

$$\boldsymbol{J}^{-1} = \begin{bmatrix} j_{11}^i & j_{12}^i & j_{13}^i \\ j_{21}^i & j_{22}^i & j_{23}^i \\ j_{31}^i & j_{32}^i & j_{33}^i \end{bmatrix} \qquad (2.19)$$

Thus, 2.9 becomes

$$\dot{\boldsymbol{\omega}} = \begin{bmatrix} j_{11}^i & j_{12}^i & j_{13}^i \\ j_{21}^i & j_{22}^i & j_{23}^i \\ j_{31}^i & j_{32}^i & j_{33}^i \end{bmatrix} \left(\begin{bmatrix} T_x \\ T_y \\ T_z \end{bmatrix} - \begin{bmatrix} c_1 \\ c_2 \\ c_3 \end{bmatrix} \right) \Leftrightarrow \qquad (2.20)$$

$$= \begin{bmatrix} j_{11}^i\left(T_x - c_1\right) + j_{12}^i\left(T_y - c_2\right) + j_{13}^i\left(T_z - c_3\right) \\ j_{21}^i\left(T_x - c_1\right) + j_{22}^i\left(T_y - c_2\right) + j_{23}^i\left(T_z - c_3\right) \\ j_{31}^i\left(T_x - c_1\right) + j_{32}^i\left(T_y - c_2\right) + j_{33}^i\left(T_z - c_3\right) \end{bmatrix} \qquad (2.21)$$

```
dot_p = Ji[0]*(T_x-C[0]) + Ji[1]*(T_y - C[1]) + Ji[2]*(T_z - C[2])
dot_q = Ji[3]*(T_x-C[0]) + Ji[4]*(T_y - C[1]) + Ji[5]*(T_z - C[2])
dot_r = Ji[6]*(T_x-C[0]) + Ji[7]*(T_y - C[1]) + Ji[8]*(T_z - C[2])
```

2.4   Linear Velocity

We define linear velocity and its components as

$$\boldsymbol{v_b} = [u \ v \ w]^T \qquad (2.22)$$

Its time derivative is

$$\dot{\boldsymbol{v}_b} = -\boldsymbol{\omega_b} \times \boldsymbol{v_b} + \frac{\boldsymbol{F_b}}{m} \tag{2.23}$$

which is equivalent to

$$\dot{u} = rv - qw + \frac{F_b x}{m} \tag{2.23a}$$

$$\dot{v} = -ru + pw + \frac{F_b y}{m} \tag{2.23b}$$

$$\dot{w} = qu - pv + \frac{F_b z}{m} \tag{2.23c}$$

```
dot_u = r*v - q*w + F_x/m
dot_v = -r*u + p*w + F_y/m
dot_w = q*u - p*v + F_z/m
```

We need to define the wind velocity, in the body frame. This is the velocity of the air-mass, moving above the ground, expressed in the body axes.

$$\boldsymbol{v_w} = [u_w \ v_w \ w_w]^T \tag{2.24}$$

The resulting relative (air)speed of the aircraft is

$$\boldsymbol{v_r} = \boldsymbol{v_b} - \boldsymbol{v_w} \tag{2.25}$$

```
u_r = u - u_w
v_r = v - v_w
w_r = w - w_w
```

Relative velocity is a very important quantity in aeronautics, as every aspect of the aircraft's aerodynamic response depends on it, rather than the inertial speed.

Based on the relative velocity, we define three more quantities:

- the angle of attack, α

- the angle of sideslip, β

- the airspeed, V_a

$$\alpha = \tan^{-1}\left(\frac{w_r}{u_r}\right) \tag{2.26a}$$

$$\beta = \sin^{-1}\left(\frac{v_r}{V_a}\right) \tag{2.26b}$$

$$V_a = \|[u_r \ v_r \ w_r]^T\| \tag{2.27}$$

Modeling of a Fixed-Wing UAV

```
    alpha = atan2(w_r,u_r)
    beta = asin(v_r/V_a)
    V_a = sqrt(u_r*u_r + v_r*v_r + w_r*w_r)
```

Using these angles, a new frame of reference can be constructed, the Stability frame $\mathcal{F}_S$. The relative speed components (expressed in the body frame) can be constructed from the airspeed (expressed in the stability frame) using the following rotation:

$$\boldsymbol{v}_r = \boldsymbol{S}^T \begin{bmatrix} V_a \\ 0 \\ 0 \end{bmatrix} \tag{2.28}$$

$$\boldsymbol{S} = \begin{bmatrix} \cos\alpha\cos\beta & \sin\beta & \sin\alpha\cos\beta \\ -\cos\alpha\sin\beta & \cos\beta & -\sin\alpha\sin\beta \\ -\sin\alpha & 0 & \cos\alpha \end{bmatrix} \tag{2.29}$$

2.5 Mass Distribution

It is useful to model the mass distribution of our aircraft. It has a nominal mass m_{nom}, placed at the center of mass, the origin of the body axes. Any extra weights, such as payloads, debris, or component detachment can be modeled with extra masses m_i. Under this definition, m_i is allowed to be negative. The overall mass and center of mass are

$$m = m_{nom} + \sum m_i \tag{2.30a}$$

$$\boldsymbol{p}_{m_{nom}} = [0\ 0\ 0]^T \tag{2.30b}$$

$$\boldsymbol{p}_{CM} = \frac{1}{m}\left(\sum \boldsymbol{p}_{m_i} m_i\right) \tag{2.31}$$

```
  m = m_nom + m_i
  p_cm_x = 1/m*(x_mi*m_i)
  p_cm_y = 1/m*(y_mi*m_i)
  p_cm_z = 1/m*(z_mi*m_i)
```

Naturally, mass additions also affect the matrix of inertia of the aircraft. A mass m_i planted at the point $p_{m_i} = [x_{m_i}, y_{m_i}, z_{m_i}]^T$ perturbs the matrix of inertia additively by

$$\Delta \boldsymbol{J}_{m_i} = \begin{bmatrix} y_{m_i}z_{m_i}m_i & -x_{m_i}y_{m_i}m_i & -x_{m_i}z_{m_i}m_i \\ -x_{m_i}y_{m_i}m_i & x_{m_i}z_{m_i}m_i & -y_{m_i}z_{m_i}m_i \\ -x_{m_i}z_{m_i}m_i & -y_{m_i}z_{m_i}m_i & x_{m_i}y_{m_i}m_i \end{bmatrix} \tag{2.32}$$

```
  J_delta_i[0] = y_mi*z_mi*m_i
  J_delta_i[1] = -x_mi*y_mi*m_i
  J_delta_i[2] = -x_mi*z_mi*m_i
  J_delta_i[3] = -x_mi*y_mi*m_i
  J_delta_i[4] = x_mi*z_mi*m_i
  J_delta_i[5] = -y_mi*z_mi*m_i
  J_delta_i[6] = -x_mi*z_mi*m_i
  J_delta_i[7] = -y_mi*z_mi*m_i
  J_delta_i[8] = x_mi*y_mi*m_i
```

In case of mass perturbations, the new matrix of inertia can be calculated and used in (2.9).

2.6 Wind

The effect of wind is often omitted in works containing simple models of UAVs, but its contribution is deciding when models are required to compare with reality, especially when it comes to fixed-wing airframes. The behaviour and performance of the aircraft is greatly affected by the movement of the air mass that it flies in and thus this movement should be taken into account.

The contribution of wind is usually modeled as an external velocity, rather than a force. This velocity is superimposed to the inertial velocity of the aircraft to extract the overall relative airspeed, which is used in aerodynamics calculations.

Two velocity components are considered: one for describing the constant wind velocity and one for producing wind turbulence. Static wind is intuitively expressed in the inertial frame, while turbulence is usually expressed in the body frame, so care is required in order to avoid confusion and errors in notation and coding.

$$\boldsymbol{v_w} = \boldsymbol{v_{ws}} + \boldsymbol{v_{wg}} \tag{2.33}$$

We denote with $\boldsymbol{v_{ws}}$ the constant wind vector in the body frame, with components.

$$\boldsymbol{v_{ws}} = \boldsymbol{R}_b [v_{ws,n}, v_{ws,e}, v_{ws,d}]^T \tag{2.34}$$

```
u_ws = (cos(theta)*cos(psi))*u_ws_I + (cos(theta)*sin(psi))*v_ws_I +
    (-sin(theta))*w_ws_I
v_ws = (sin(phi)*sin(theta)*cos(psi)-cos(phi)*sin(psi))*u_ws_I + (
    sin(phi)*sin(theta)*sin(psi)+cos(phi)*cos(psi))*v_ws_I + (sin(phi
    )*cos(theta))*w_ws_I
```

```
w_ws = (cos(phi)*sin(theta)*cos(psi)+sin(phi)*sin(psi))*u_ws_I + (
    cos(phi)*sin(theta)*sin(psi)-sin(phi)*cos(psi))*v_ws_I + (cos(phi
    )*cos(theta))*w_ws_I
```

Models for both static wind (in the inertial frame) $\boldsymbol{v_{ws}}$ and wind gusts $\boldsymbol{v_{wg}}$ can be found in Section 4.3.

Chapter 3

Dynamic Equations

In this chapter the forces and moments exerted on the aircraft will be presented. The main dynamic components are gravity, aerodynamic reactions and propulsion (also referred to as thrust).

$$\boldsymbol{F}_b = \boldsymbol{F}_g + \boldsymbol{F}_a + \boldsymbol{F}_t \tag{3.1}$$

```
F_x = F_g_x + F_a_x + F_t_x
F_y = F_g_y + F_a_y + F_t_y
F_z + F_g_z + F_a_z + F_t_z
```

Naturally, we consider that gravity does not exert moments on the rigid body aircraft.

$$\boldsymbol{T}_b = \boldsymbol{T}_{a,tot} + \boldsymbol{T}_{t,tot} \tag{3.2}$$

```
T_x = T_atot_x + T_ttot_x
T_y = T_atot_y + T_ttot_y
T_z = T_atot_z + T_ttot_z
```

Before proceeding to any definitions, it is worth mentioning the control input variables. In normal airplane configurations, there are four control dimensions which the pilot can affect. These correspond to three sets of control surfaces (aileron, elevator and rudder) and the throttle command. The notation for these control variables is $\delta_a, \delta_a, \delta_t, \delta_r$. Essentially, these are the input variables to the aircraft model. δ_a, δ_e, and δ_r are usually expressed in degrees of deflection from the neutral (zero) angle and δ_t is normalized in the (0,1) range.

Conventions for the positive direction of each control surface are not always consistent. In this text, the proposed positive direction of a control surface is the one which results in a positive moment around each primary axis (aileron - roll right, elevator - pitch up, rudder - yaw right).

3.1 Gravity

Initially, we can assume a constant value for the acceleration of gravity, $g_0 = 9.805416 m/s^2$ [1, p. 8]. The magnitude of the acceleration of gravity normally varies with altitude and geodetic coordinates, but a constant value is a valid approach for low altitude flight; unmodeled components are negligible to an adequate accuracy. If a more detailed gravity model is required (for example, in flights with vertical variance in the scale of kilometers), the reader can turn to Section 4.1. The orientation of the gravity vector is always vertical, towards the center of the Earth, thus in the z-direction in the NED frame.

$$\boldsymbol{F}_g = \boldsymbol{R}_b \begin{bmatrix} 0 \\ 0 \\ mg \end{bmatrix} \tag{3.3}$$

$$F_{gx} = -\sin\theta \; mg \tag{3.3a}$$
$$F_{gy} = \sin\phi\cos\theta \; mg \tag{3.3b}$$
$$F_{gz} = \cos\phi\cos\theta \; mg \tag{3.3c}$$

```
F_g_x = -sin(theta)*m*g
F_g_y = sin(phi)*cos(theta)*m*g
F_g_z = cos(phi)*cos(theta)*m*g
```

$$g = g_0 \tag{3.4}$$

3.2 Aerodynamics

This is the defining part of the flight characteristics of an airplane. The aerodynamic response of the airplane is crucial for its stability as well as its maneuverability. Aerodynamic forces are presented in two frames of reference. The first is the body frame, whose corresponding forces, $\boldsymbol{F_a}$ are used for kinematic calculations.

$$\boldsymbol{F_a} = \begin{bmatrix} F_{ax} \\ F_{ay} \\ F_{az} \end{bmatrix} \tag{3.5}$$

Aerodynamic forces are considered to be exerted, under normal operation, at the *center of lift* ($\boldsymbol{p}_{CoL}$), a point located on the symmetry plane of the aircraft at one-quarter of the main wing chord.

However, for both historical and practical reasons, the flight characteristics of the airplane and the resulting forces (lift, drag and sideforce) are expressed in the stability frame (see 2.29). Models of aircraft aerodynamics are also parametrized so as to predict the aerodynamic forces in the stability frame as well.

$$\boldsymbol{F_s} = \begin{bmatrix} -F_D \\ F_Y \\ -F_L \end{bmatrix} \tag{3.6}$$

Thus, we can obtain $\boldsymbol{F_a}$ via the equation

$$\boldsymbol{F_a} = \boldsymbol{S}^T \boldsymbol{F_s} \tag{3.7}$$

We remind that

$$\boldsymbol{S} = \begin{bmatrix} \cos\alpha\cos\beta & \sin\beta & \sin\alpha\cos\beta \\ -\cos\alpha\sin\beta & \cos\beta & -\sin\alpha\sin\beta \\ -\sin\alpha & 0 & \cos\alpha \end{bmatrix}$$

$$F_{ax} = -\cos\alpha F_D - \cos\alpha\sin\beta F_Y + \sin\alpha F_L \tag{3.7a}$$
$$F_{ay} = -\sin\beta F_D + \cos\beta F_Y \tag{3.7b}$$
$$F_{az} = -\sin\alpha\cos\beta F_D - \sin\alpha\sin\beta F_Y - \cos\alpha F_L \tag{3.7c}$$

```
F_a_x = -cos(alpha)*F_D - cos(alpha)*sin(beta)*F_Y + sin(alpha)*F_L
F_a_y = -sin(beta)*F_D + cos(beta)*F_Y
F_a_z = -sin(alpha)*cos(beta)*F_D - sin(alpha)*sin(beta)*F_Y - cos(
    alpha)*F_L
```

Aerodynamic moments need not be modeled in the stability frame. However, forces are generally not applied on the center of gravity of the aircraft, thus we need to model the moment they apply on it separately. Sources of such additional moments are the stability margin (how much forward than the center of lift lies the center of mass), height difference between center of mass and center of lift (for example in a high-wing aircraft) and mass additions and subtractions to the airframe.

$$\boldsymbol{T_{a,tot}} = \begin{bmatrix} T_{ax} \\ T_{ay} \\ T_{az} \end{bmatrix} + (\boldsymbol{p}_{CoL} - \boldsymbol{p}_{CG}) \times \boldsymbol{F_a} \tag{3.8}$$

$$T_{ax,tot} = T_{ax} - dzF_{ay} + dyF_{az} \tag{3.8a}$$
$$T_{ay,tot} = T_{ay} + dzF_{ax} - dxF_{az} \tag{3.8b}$$
$$T_{az,tot} = T_{az} - dyF_{ax} + dxF_{ay} \tag{3.8c}$$

```
dx = p_cl_x - p_cm_x
dy = p_cl_y - p_cm_y
dz = p_cl_z - p_cm_z
T_atot_x = T_a_x - dz*F_a_y + dy*F_a_z
T_atot_y = T_a_y + dz*F_a_x - dx*F_a_z
T_atot_z = T_a_z - dy*F_a_z + dx*F_a_y
```

The next step in exploring the aerodynamic model is the definition of dynamic pressure. This quantity expresses the pressure exerted by the air moving around the airplane per unit of surface. It is proportional with the density of the air and with the square of the airspeed. Dynamic pressure is a crucial scaling factor for the rest of the aerodynamic equations

$$\bar{q} = \frac{1}{2}\rho V_a^2 \tag{3.9}$$

```
q_bar = 0.5*rho*V_a*V_a
```

The air density, ρ, is dependent upon altitude. Its sea level value ($\rho_0 = 1.225 kg/m^3$) is often used as an approximate value for low-altitude flight, but if needed, accurate atmospheric models are provided in Section 4.2.

We are now able to express the force components as the product of dynamic pressure, the wing surface S, and the aerodynamic coefficients of lift, drag and sideforce, C_L, C_D, C_Y. It is very important to appreciate that these coefficients are not constant values; instead, they are functions of the state of the flying body, albeit their dependence from some state variables is more dominant than others. A more detailed explanation is given further down.

$$F_D = \bar{q}SC_D \tag{3.10a}$$
$$F_Y = \bar{q}SC_Y \tag{3.10b}$$
$$F_L = \bar{q}SC_L \tag{3.10c}$$

```
F_D = q_bar*S*C_D
F_Y = q_bar*S*C_Y
F_L = q_bar*S*C_L
```

$$C_D = C_D(V_a, \alpha, q, \delta_e) \tag{3.11a}$$
$$C_Y = C_Y(V_a, \beta, p, r, \delta_a, \delta_r) \tag{3.11b}$$
$$C_L = C_L(V_a, \alpha, q, \delta_e) \tag{3.11c}$$

The aerodynamic moments are defined in a similar fashion, with the additional inclusion of wingspan b and wing chord c. The notation for the moment coefficients may vary from source to source.

$$T_{ax} = \bar{q}SbC_l \tag{3.12a}$$
$$T_{ay} = \bar{q}ScC_m \tag{3.12b}$$
$$T_{az} = \bar{q}SbC_n \tag{3.12c}$$

```
T_a_x = q_bar*S*b*C_l
T_a_y = q_bar*S*c*C_m
T_a_z = q_bar*S*b*C_n
```

$$C_l = C_l(V_a, \beta, p, r, \delta_a, \delta_r) \tag{3.13a}$$

$$C_m = C_m(V_a, \alpha, q, \delta_e) \tag{3.13b}$$

$$C_n = C_n(V_a, \beta, p, r, \delta_a, \delta_r) \tag{3.13c}$$

Finally, a model for the aerodynamic coefficients is provided. Undoubtedly, the most common and established approach is to use multivariable polynomials which are linear with respect to their coefficients. This representation lends itself nicely for parameter identification techniques, such as least-squares flavours, very common in real-world aircraft design and testing.

$$C_D = C_{D0} + C_{D\alpha}\alpha + C_{Dq}\frac{c}{2V_a}q + C_{D\delta_e}\delta_e \tag{3.14a}$$

$$C_Y = C_{Y0} + C_{Y\beta}\beta + C_{Yp}\frac{b}{2V_a}p + C_{Yr}\frac{b}{2V_a}r + C_{D\delta_a}\delta_a + C_{Y\delta r}\delta_r \tag{3.14b}$$

$$C_L = C_{L0} + C_{L\alpha}\alpha + C_{Lq}\frac{c}{2V_a}q + C_{L\delta_e}\delta_e \tag{3.14c}$$

```
C_D = C_D0 + C_Dalpha*alpha + C_Dq*c*0.5/V_a*q + C_Ddeltae*deltae
C_Y = C_Y0 + C_Ybeta*beta + C_Yp*b*0.5/V_a*p + C_Yr*b*0.5/V_a*r +
    C_Ddeltaa*deltaa + C_Ydeltar*deltar
C_L = C_L0 + C_Lalpha*alpha + C_Lq*c*0.5/V_a*q + C_Ldeltae*deltae
```

$$C_l = C_{l0} + C_{l\beta}\beta + C_{lp}\frac{b}{2V_a}p + C_{lr}\frac{b}{2V_a}r + C_{l\delta_a}\delta_a + C_{l\delta_r}\delta_r \tag{3.15a}$$

$$C_m = C_{m0} + C_{m\alpha}\alpha + C_{mq}\frac{c}{2V_a}q + C_{m\delta_e}\delta_e \tag{3.15b}$$

$$C_n = C_{n0} + C_{n\beta}\beta + C_{np}\frac{b}{2V_a}p + C_{nr}\frac{b}{2V_a}r + C_{n\delta_a}\delta_a + C_{n\delta_r}\delta_r \tag{3.15c}$$

```
C_l = C_l0 + C_lbeta*beta + C_lp*b*0.5/V_a*p + C_lr*b*0.5/V_a*r +
    C_ldeltaa*deltaa + C_ldeltar*deltar
C_m = C_m0 + C_malpha*alpha + C_mq*c*0.5/V_a*q + C_mdeltae*deltae
C_n = C_n0 + C_nbeta*beta + C_np*b*0.5/V_a*p + C_nr*b*0.5/V_a*r +
    C_ndeltaa*deltaa + C_n_deltar*deltar
```

The coefficients which correspond to state variables ($C_{D\alpha}$, C_{Dq}, $C_{Y\beta}$, C_{Yp}, C_{Yr}, $C_{L\alpha}$, C_{Lq}, $C_{l\beta}$, C_{lp}, C_{lr}, $C_{m\alpha}$, C_{mq}, $C_{n\beta}$, C_{np}, C_{nr}) in most cases have values such that the

resulting forces and moments tend to revert the aircraft to straight and level flight. Hence they are called *stability derivatives*.

On the other hand, coefficients which correspond to the input variables ($C_{D\delta e}$, $C_{D\delta a}$, $C_{Y\delta r}$, $C_{L\delta e}$, $C_{l\delta_a}$, $C_{l\delta_r}$, $C_{m\delta_e}$, $C_{n\delta_a}$, $C_{n\delta_r}$) describe how the aircraft responds to control inputs and are hence called *control derivatives*.

Discuss about $C_{L\alpha}$ shape

Not all of the above derivatives need to be used in the formulation of the aerodynamic model of a plane. Some of them might be statistically insignificant for certain airframes [9]. On the other hand, longitudinal quantities usually do not incorporate coefficients of lateral quantities and vice versa. This is in-line with the effort of decoupling the aircraft dynamics into a longitudinal and lateral plane, as much as possible, but there also are physical reasons, stemming from the aircraft geometry.

3.3   Propulsion

The devices which produce propulsion force in an aircraft can be termed *thrusters*, in general. In the case of fixed-wing aircraft, most of the times thrusters take the form of a single propeller driven by a motor, usually acting upon the longitudinal axis of the aircraft, placed either in the front or the back of the fuselage. This discussion mainly draws from [2, p. 127] but extends its contents from other sources to adapt to an electric power plant. Thruster placement does not have an impact on the set of equations which form the thruster model, even in the case of twin-propeller configurations, mounted on the wings.

The propulsion force, expressed in the body-frame is declared as

$$\boldsymbol{F}_t = \begin{bmatrix} F_{tx} \\ F_{ty} \\ F_{tz} \end{bmatrix} \tag{3.16}$$

Usually, thrust is considered to be produced only along the body x-axis, however, this approach may lack realism: it is not uncommon for the propeller to be mounted slightly tilted right and downwards, in order to minimize the counter-moment it produces and which affects the aircraft stability negatively.

However, under the simplification that the propeller is aligned with the body frame x-axis, the following is also true:

$$F_{ty} = 0 \tag{3.16a}$$
$$F_{tz} = 0 \tag{3.16b}$$

```
F_t_y = 0
F_t_z = 0
```

Naturally, the motor and propeller produce moments. Similarly to the aerodynamic moment analysis, we also have to take into account the displacement of the trust vector from the x-axis of the body frame.

$$\boldsymbol{T_t} = \begin{bmatrix} T_{tx} \\ T_{ty} \\ T_{tz} \end{bmatrix} + (\boldsymbol{p}_{prop} - \boldsymbol{p}_{CG}) \times \boldsymbol{F}_p \tag{3.17}$$

$$T_{tx,tot} = T_{tx} - dzF_{ty} + dyF_{tz} \tag{3.17a}$$
$$T_{ty,tot} = T_{ty} + dzF_{tx} - dxF_{tz} \tag{3.17b}$$
$$T_{tz,tot} = T_{tz} - dyF_{tx} + dxF_{ty} \tag{3.17c}$$

```
dx = p_prop_x - p_cm_x
dy = p_prop_y - p_cm_y
dz = p_prop_z - p_cm_z
T_ttot_x = T_t_x - dz*F_t_y + dy*F_t_z
T_ttot_y = T_t_y + dz*F_t_x - dx*F_t_z
T_ttot_z = T_t_z - dy*F_t_z + dx*F_t_y
```

We opt to consider in our model only the aforementioned counter-moment produced in the x-axis by the propeller and motor, and not gyroscopic effects caused by the spinning propeller disc:

$$T_{ty} = 0 \tag{3.17d}$$
$$T_{tz} = 0 \tag{3.17e}$$

```
T_t_y = 0
T_t_z = 0
```

With the aforementioned assumptions, the moment equations can be simplified into

$$T_{ax,tot} = T_{tx} \tag{3.17f}$$
$$T_{ay,tot} = dzF_{ax} \tag{3.17g}$$
$$T_{az,tot} = -dyF_{ax} \tag{3.17h}$$

```
T_ttot_x = T_t_x
T_ttot_y = dz*F_a_x
T_ttot_z = -dy*F_a_x
```

In the next subsection, a simplified model of a lumped thruster will be presented, as presented in [5]. Afterwards, more detailed models will be presented, where the propeller model will be decoupled from the motor model. This enables the possibility to take advantage of the large amount of resources on propeller data and use them independently of the motor selection. The correct selection of the proper propeller for a given motor and vice versa can also be studied with this approach. Models for both electric and internal combustion motors will be presented.

Simplified Thruster

In preliminary simulation and control analyses, simplified models are often preferred. When it comes to airplane thrusters, the core behavioural characteristics that should be captured in any level of detail should be the maximum available thrust, as well as the reduction of produced thrust as the airspeed increases. In [5] such a model is provided, presented below.

$$F_{tx} = \rho k_{F1} * \left((k_{F2}\delta_t)^2 - V_a^2 \right) \tag{3.18}$$

$$F_{ty} = 0 \tag{3.19}$$

$$F_{tz} = 0 \tag{3.20}$$

```
F_t_x = rho*k_F1*(k_F2*k_F2*deltat*deltat - V_a*V_a)
F_t_y = 0
F_t_z = 0
```

$$T_{tx} = - (k_T\delta_t)^2 \tag{3.21}$$

$$T_{ty} = 0 \tag{3.22}$$

$$T_{tz} = 0 \tag{3.23}$$

```
T_t_x = -k_T*k_T*deltat*deltat
T_t_y = 0
T_t_z = 0
```

δt is the motor control input. k_{F2} is the pitch speed of the propeller, i.e. the airspeed at which it can no longer produce any at maximum input and has velocity units. By extension, $\rho k_{F1} k_{F2}^2$ is the maximum force the thruster can produce, which occurs at maximum input and zero airspeed.

k_T^2 is the maximum counter-torque that the motor produces. The square proportionality reflects the real-life, non-linear behaviour of propellers in general.

Propeller Model

If the model of Section 3.3 is not detailed enough,a clear separation between the propeller and motor models is possible. In this section a standard propeller model is presented, commonly found in literature and in the following sections various motor models are laid out.

Much like the aerodynamics of the airplane lifting surfaces, propeller thrust is dependent upon a coefficient function (C_t), the air density (ρ) and its scale (propeller diameter D). Additionally, it is proportional to the square of its rotational speed n, which is expressed in revolutions per second. If SI units need be employed then n can be easily swapped for ω_{prop} in $\mathrm{rad\,s^{-1}}$ (3.25).

$$F_{tx} = C_t \rho n^2 D^4 \tag{3.24}$$

$$n_{prop} = \frac{\omega_{prop}}{2\pi} \tag{3.25}$$

```
F_t_x = C_t*rho*n*n*D*D*D*D
n_prop = w_prop/2/pi
```

This time, the coefficient of thrust function has only one variable, the *advance ratio* (J). This quantity is the ratio of the aircraft airspeed to the speed the propeller "screws" itself into the air volume. It is a means to quantify how efficiently the propeller forces itself into the air, in other words, its operational state. C_T generally doesn't have a simple shape. It is usually given by propeller manufacturers as a data set, which peaks at the nominal advance ratio and falls off at either side of the advance ratio range. This function can adequately model propeller stall, as well as the windmilling effect.

$$J = \frac{V_a}{nD} \tag{3.26}$$

$$C_t = C_t(J) \tag{3.27}$$

```
Jar = V_a/n/D
```

C_t can be described as a polynomial of J, with a degree ranging from 3-6. A spline representation is also possible. Typical shapes of the C_t curve can be seen in Figure 3.1, for propellers with increasing pitch, ranging from 0° to 40°. Image taken from [2].

In a similar fashion, there is an expression for the power that is consumed by the propeller in order to produce thrust and it uses a coefficient of power (C_p). Again, typical shapes for the curve C_p can be seen in Figure 3.2. Image taken from [2].
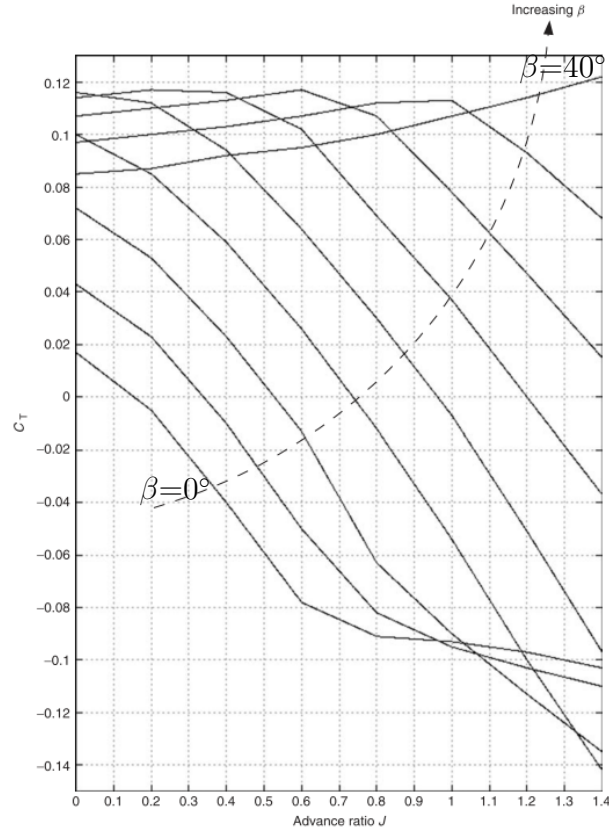
Figure 3.1: Coefficient of Thrust as a function of Advance Ratio

$$P_{prop} = C_p \rho n^3 D^5 \tag{3.28}$$
$$C_p = C_p(J) \tag{3.29}$$

```
P_{prop} = C_p*rho*n*n*n*D*D*D*D*D
```

A detail included in this model, not mentioned in most resources, is the equation which describes how the rotational speed of the propeller changes transiently in time. This is a differential equation of the rotational speed as a function of the difference between the available power from the motor (P_{mot}) and the power consumed by the propeller. A necessary parameter is the sum of the moments of inertia along the x-axis of the engine and the propeller, denoted as J_{prop} and J_{mot}.

$$\dot{n}_{prop} = \frac{1}{J_{prop} + J_{mot}} \frac{P_{mot} - P_{prop}}{n_{prop}} \tag{3.30}$$

```
dot_n_prop = 1/(J_prop + J_mot)*(P_mot - P_prop)
```
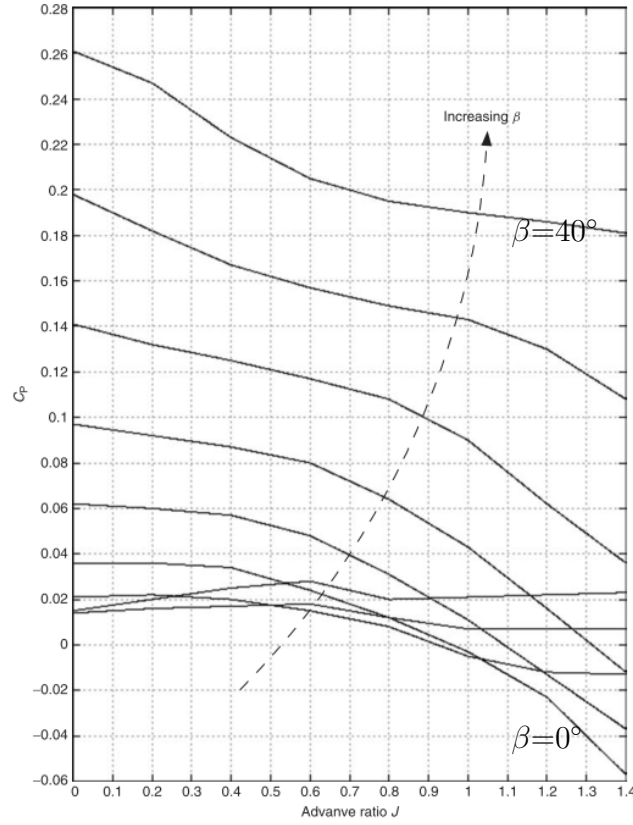
Figure 3.2: Coefficient of Powerust as a function of Advance Ratio

Finally, the expression of propeller moment is simply derived from the ratio of the propeller power over the propeller rotational speed.

$$T_{tx} = \frac{P_{prop}}{\omega_{prop}} \tag{3.31}$$

```
T_t_x = P_prop / w_prop
```

Electric Motor Model

The most wide-spread motor used in small UAVs is the brushless outrunner permanent magnet electrical motor. Commonly a 3-constant model is used, but for the sake of completeness, a 4-constant model will be used here, as presented in [7]. The equivalent circuit can be seen in Figure 3.3, form the same source.

The input to the motor is the driving voltage, V_{mot} and the output is the output power, P_{mot}. Naturally, if there is a direct-drive configuration between the motor and the propeller, the motor rotational speed (n_{mot}, in revolutions per second) is the same as that of the propeller.
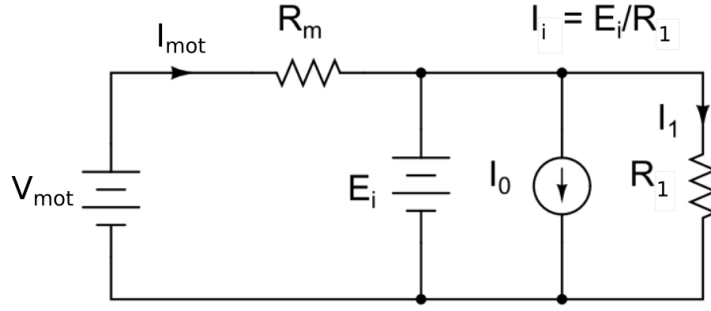
Figure 3.3: Coefficient of Thrust as a function of Advance Ratio

```
n_prop = n_mot
```

$$n_{mot} = K_v E_i \tag{3.32}$$

$$E_i = V_{mot} - I_{mot} R_m \tag{3.33}$$

$$P_{mot} = E_i I_i \tag{3.34}$$

$$I_i = I_{mot} - I_0 - \frac{E_i}{R_1} \tag{3.35}$$

$$P_{elec} = V_{mot} I_{mot} \tag{3.36}$$

```
n_mot = K_v*E_i
E_i = V_mot - I_mot*R_m
P_mot = E_i*I_i
I_i = I_mot - I_0 - E_i/R_1
P_elec = V_mot*I_mot
```

Battery and Electronic Speed Controller

Finally, an expression for the overall combination of the battery and ESC is given.

- V_{bat} is the internal battery voltage

- R_{bat} is the battery internal resistance

- R_S is the ESC in-line resistance

- δ_t is the throttle command, essentially modulating the output voltage

$$V_{mot} = (V_{bat} - I_{mot}(R_{bat} + R_S))\delta_t \tag{3.37}$$

```
V_mot = (V_bat - I_mot*(R_bat + R_S))*deltat
```

Chapter 4

Miscellaneous Models

During simulation, other models are required to complement the aircraft mathematical description. These describe the rest of the environment and its evolution and are necessarily included, if the interactions of the aircraft with its environment are to be modeled. The shape of the Earth, its gravity and magnetic field, the atmosphere as well as the wind are topics discussed in this chapter.

4.1   Earth Model

This section draws from [13], specifically chapter 3 and equations of p. 7.5, regarding the shape of the Earth. According to the WGS-84, the Earth is modeled as an ellipsoid which is flatter on the poles and symmetric on the z-axis (the Earth's rotation axis). The semi-major axis is

$$a = 6\,378\,137\,\text{m} \tag{4.1}$$

and the flattening, defined as

$$f = \frac{a - b}{a} \tag{4.2}$$

is equal to

$$\frac{1}{f} = 298.257222101 \tag{4.3}$$

b is the semi-minor axis of the ellipsoid and is calculated from the above equations and is equal to

$$b = 6\,356\,752.3142\,\text{m} \tag{4.4}$$

The first eccentricity, e, is defined as

$$e^2 = 2f - f^2 \tag{4.5}$$

With these constants available, for any given point on the surface of the Earth with latitude ϕ, we can calculate the radius of curvature in the prime vertical

$$R_N = \frac{a}{\sqrt{1 - e^2 \sin^2 \phi}} \tag{4.6}$$

and the curvature in the meridian

$$R_M = \frac{a(1 - e^2)}{(1 - e^2 \sin^2 \phi)^{3/2}} \tag{4.7}$$

Finally, a small change of latitude $\Delta\phi$ causes a shift in the north-south direction

$$\Delta n = R_M \sin \Delta\phi \tag{4.8}$$

and a small change of longitude $\Delta\lambda$ causes a shift in the east-west direction

$$\Delta e = R_N \sin \Delta\lambda \tag{4.9}$$

For such small angles (in the order of hundredths of a degree), the simplification $\sin \Delta\phi = \Delta\phi$ (in radians) might be acceptable.

For reference, at a latitude of 45°, a change of 0.01° to the North corresponds to a distance of 1111.318 m and the same change Eastwards corresponds to 1115.062 m.

Sidenote: As of writing, the Google Earth 7.1.2 application for Linux reports a distance of about 1113m between the coordinates (45.00,00.00) and (45.01,00.00) and (curiously) a distance of about 788m(!) between the coordinates (45.00,00.00) and (45.00,00.01). Until further investigation, this results seems to be erroneous.

In case simpler calculations are required, one could use the geometric mean of the semi-major and semi-minor axis

$$\bar{R} = \sqrt{a * b} \tag{4.10}$$

and multiply it by the change in angle, regardless of direction.

$$\Delta n = \bar{R}\Delta\phi \tag{4.11}$$

For the previous example, the above equation yields 1111.327m, which is very acceptable for many applications.

> Add a set of equations for the reverse procedure, from Δx to $\Delta\phi$.

Regarding altitude, we consider that the vertical distance from the surface of the ellipsoid h is available. Since the local NED frame is placed at the starting altitude, this altitude (h_0) should be used to initialize the frames. One could take altitude into account when calculating Cartesian displacements in the NED frame. This is as simple as adding altitude to the local Earth radius. This is demonstrated below.

Summing up, we do the following steps to convert from geodetic coordinates to local coordinates:

1. Note the starting coordinates ϕ_0, λ_0 and altitude h_0

2. Calculate the radii of curvature $R_N(\phi_0)$ and $R_M(\phi_0)$

For each GPS reading (ϕ, λ, h)

1. Calculate the differences $\Delta\phi = \phi - \phi_0$, $\Delta\lambda = \lambda - \lambda_0$ and $\Delta h = h - h_0$

2. Calculate $n = (R_M + h)\sin\Delta\phi$

3. Calculate $e = (R_N + h)\sin\Delta\lambda$

4. Calculate $d = -\Delta h$

In a different approach, we can treat the state of the GPS coordinates (ϕ, λ, h) as a dynamic system, which is driven by $\dot{n}$, $\dot{e}$ and $\dot{d}$. Although more complicated, this procedure is suitable in cases where the trajectory of the aircraft is expected to arc around the Earth. In these cases the Flat Earth assumption breaks rendering the previous calculations invalid.

Write the coordinate evolution system.

4.2   Atmosphere Model

The primary resource for atmospheric models is [1]. This technical report is the most accessible and adequately complete document among its "competitors". It provides models for all of the components of the atmosphere, ranging from temperature gradients to molecular synthesis of the air. It partitions the atmosphere into several layers, but we are interested only in the first one, spanning from $0\,\mathrm{m}$ to approximately $11\,\mathrm{km}$. This range is adequate for the majority of UAV operations.

Note: The following discussion uses the gravitational model from [1, eq. 17]. This model differs from the one presented in [13] in a noticeable way. [1] uses the *Standard Gravity* for the gravitational acceleration on the surface of the Earth, established by the International Committee on Weights and Measures in 1901.

$$g_0 = 9.80665 \ m/s^2 \tag{4.12}$$

This number is used uniformly for all latitudes. It is known that this is a simplification. However, we can proceed to the rest of the calculations and if need arises, switch g_0 for the more detailed model from [13, eq. 4-1].

Additionally, the US Standard Atmosphere gravity model with respect to altitude uses the inverse square law for gravity decay

$$g(z) = g_0 \left(\frac{r_0}{r_0 + z}\right) \tag{4.13}$$

```
g = g_0*r_0/(r_0+z)
```

where

- z is the geometric altitude above the ellipsoid surface, as reported by GPS systems.

- r_0 is the radius of the Earth at a latitude where g_0 takes its standard value of $9.806\,65\,\mathrm{m\,s^{-2}}$. Considering a constant g_0 for all latitudes, r_0=6356.766 km.

The respective altitude model in WGS-84 is given in equation (4-3), for relatively low altitudes. Again, one can opt to use that model.

Where all this matters, is in the definition of the *geopotential altitude*, h. This is expressed in *geopotential meters* (m'), a unit of altitude, lifting a mass by which, always requires the same amount of work, no matter at which altitude this work is performed. Essentially, this expresses how easier it gets to lift masses in the weakening gravity as altitude increases and, in turn, this affects how less densely atmosphere is packed as altitude increases.

$$h = \frac{1}{g_0} \int_0^z g \cdot dz \tag{4.14}$$

Combining equations 4.12, 4.13 and 4.14 we get the following conversion expressions between geometric and geopotential altitude

$$h = \frac{r_0 \cdot z}{r_0 + z} \tag{4.15}$$

$$z = \frac{r_0 \cdot h}{r_0 - h} \tag{4.16}$$

```
h = r_0*z/(r_0 + z)
z = r_0*h/(r_0 + h)
```

Next, we need to include a temperature model as a function of altitude.

$$T = T_0 + L_0 \cdot (h - h_0) \tag{4.17}$$

```
T = T_0 + L_0*(h - h_0)
```

where

- h_0 is the initialization altitude.

- T_0 is the temperature at our initialization altitude. Its nominal value at sea-level is $288.15\,\mathrm{K}$, but having an on-site measurement in real time is more accurate.

- $L_0 = -0.0065\,\mathrm{K\,m^{-1}}$ is the temperature gradient.

The equation above describes how temperature drops as altitude increases.

Finally, we can express the variation of barometric pressure as a function of geopotential altitude

$$P = P_0\left(\frac{T_0}{T(h)}\right)^{\left(\frac{g_0\cdot M_0}{R^*\cdot L_0}\right)} \tag{4.18}$$

```
P = P_0*pow(T_0/T,g_0*M_0/R_star/L_0)
```

where

- P_0 is the pressure at our initialization altitude. According to the US Standard Atmosphere, at sea-level its value is $P_0 = 101\,325\,\mathrm{N\,m^{-2}} = 1013.25\,\mathrm{mbar}$, but again, real time on site measurements are preferred.

- $M_0 = 0.028\,964\,4\,\mathrm{kg\,mol^{-1}}$ is the mean molecular weight of the air.

- $R^* = 8.314\,32\,\mathrm{N\,m\,mol^{-1}\,K^{-1}}$ is the gas constant.

Most importantly, one can solve this equation for h and obtain the geopotential altitude by measuring the barometric pressure.

$$h = \frac{T_0}{L_0}\left(\left(\frac{P}{P_0}\right)^{\frac{g_0\cdot M_0}{R^*\cdot L_0}} - 1\right) + h_0 \tag{4.19}$$

```
h = T_0/L_0*(pow(P/P_0,g_0*M_0/R_star/L_0)-1) + h_0
```

Air density can be obtained from the air pressure model

$$\rho = \frac{P\cdot M_0}{R^*\cdot T} \tag{4.20}$$

```
rho = P*M_0/R_star/T
```

4.3 Wind Model

Wind models are mostly useful for validation of control schemes under simulated disturbances. This section extends the discussion of Section 2.6.

Usually we consider the vertical component of the wind to be zero ($v_{ws,d} = 0$), but this is not true in environments such as mountain slopes or in regions with thermal currents.

A useful expression for constant wind is:

$$\boldsymbol{v_{ws}} = \boldsymbol{R}_b^T V_{ws}[-\cos\theta_w, -\sin\theta_w, 0]^T \tag{4.21}$$

where V_{ws} is the wind overall magnitude (in m/s) and θ_w is the wind direction (0° for North wind)

```
u_ws = (cos(theta)*cos(psi))*(-cos(theta_wind)*V_ws) + (cos(theta)*
   sin(psi))*(-sin(theta_wind)*V_ws)
v_ws = (sin(phi)*sin(theta)*cos(psi)-cos(phi)*sin(psi))*(-cos(
   theta_wind)*V_ws) + (sin(phi)*sin(theta)*sin(psi)+cos(phi)*cos(
   psi))*(-sin(theta_wind)*V_ws)
w_ws = (cos(phi)*sin(theta)*cos(psi)+sin(phi)*sin(psi))*(-cos(
   theta_wind)*V_ws) + (cos(phi)*sin(theta)*sin(psi)-sin(phi)*cos(
   psi))*(-sin(theta_wind)*V_ws)
```

This allows us to introduce an altitude model for the wind magnitude, commonly known as the Power Law:

$$V_{ws} = V_{ws,h_r} \left(\frac{h}{h_r}\right)^\alpha \tag{4.22}$$

```
V_ws = V_ws_ref*pow(h/h_ref,exp_Hell)
```

This formula describes the increase of the wind magnitude as an exponential function of the altitude, given a measurement of wind magnitude V_{ws,h_r} at altitude h_r. α is the Hellmann exponent (roughness exponent), which describes the wind shear effect. Commonly, surface wind magnitude measurements are available for the altitude of 10m, so the above formula becomes

$$V_{ws} = V_{ws,h_{10}} \left(\frac{h}{h_{10}}\right)^\alpha \tag{4.23}$$

Values for α vary with terrain morphology and wind turbulence. Some indicative values can be found in references [3], [14], [18], [19], but it is also claimed that the "1/7th power law" (using a value $\alpha = 1/7$) is an adequate approximation for most purposes. It should be noted, however, that most of the reviewed studies where oriented towards wind farm applications and wind models where validated up to a few hundred meters above ground.

The following table is pulled from [3].

Landscape type	Friction coefficient α
Lakes, ocean and smooth hard ground	0.1
Grasslands (ground level)	0.15
Tall crops, hedges and shrubs	0.20
Heavily forested land	0.25
Small town with some trees and shrubs	0.3
City areas with high rise buildings	0.4

Table 4.1: Hellmann Exponent Values over Various Terrain

An alternative model for wind shear can be found in [12].

Wind gusts can be modeled using Dryden transfer functions, as presented in [12], [4], [11] and [5] . Time responses can be generated by feeding unit variance white noise in the following filters. Note that airspeed is a parameter for these functions, but it can be replaced with the mean or cruise airspeed of the aircraft.

$$
\boldsymbol{V_{wg}}(s) = \begin{bmatrix} \sigma_u \sqrt{\frac{2V_a}{\pi L_u}} \frac{1}{s + \frac{V_a}{L_u}} \\ \sigma_v \sqrt{\frac{3V_a}{\pi L_v}} \frac{s + \frac{V_a}{\sqrt{3}L_v}}{(s + \frac{V_a}{L_u})^2} \\ \sigma_w \sqrt{\frac{3V_a}{\pi L_w}} \frac{s + \frac{V_a}{\sqrt{3}L_w}}{(s + \frac{V_a}{L_w})^2} \end{bmatrix}
\tag{4.24}
$$

During discrete implementation of the transfer functions, since first and second order functions are used, past values of the wind gusts are maintained and used.

```
u_dg = w_dg_prev*(1 - V_a/L_u*dt) + sigma_u*sqrt(1*V_a/(pi*L_u))*dt*
    noise
V_dg[1] = -pow(V_a/L_u,2)*dt*V_dg_prev[0] + V_dg_[1] + sigma_u*sqrt
    (3*V_a/(pi*L_u))*V_a/(sqrt(3)*L_u)*dt*noise
V_dg[0] = (1 - 2*V_a/L_u*dt)*V_dg_prev[0] + dt*V_dg_prev[1] +
    sigma_u*sqrt(3*V_a/(pi*L_u))*dt*noise
v_dg = V_dg[0]
W_dg[1] = -pow(V_a/L_w,2)*dt*W_dg_prev[0] + W_dg_[1] + sigma_w*sqrt
    (3*V_a/(pi*L_w))*V_a/(sqrt(3)*L_w)*dt*noise
W_dg[0] = (1 - 2*V_a/L_w*dt)*W_dg_prev[0] + dt*W_dg_prev[1] +
    sigma_w*sqrt(3*V_a/(pi*L_w))*dt*noise
w_dg = W_dg[0]
```

Typical values for the transfer function parameters for a small UAV can be found in [10] and are copied below.

Description	altitude (m)	L_u (m)	L_w (m)	σ_u (m/s)	σ_w (m/s)
low altitude, light turbulence	50	200	50	1.06	0.7
low altitude, moderate turbulence	50	200	50	2.12	1.4
medium altitude, light turbulence	600	533	533	1.5	1.5
medium altitude, moderate turbulence	600	533	533	3.0	3.0

Table 4.2: Gust Field Properties

Chapter 5

Sensory Equipment Equations

In this chapter, the equations that describe the measurements of the various quantities and states via hardware sensors are laid out. Sensors often times use complicated physical phenomena to obtain a measurement of the desired quantity and sometimes the conversion process isn't straightforward. An effort to document relevant information is done here. No effort to model measurement errors is done here. Most of the following device descriptions correspond to their MEMS versions.

5.1   Inertial Measurements

The first and perhaps most used family of sensors in robotics are the inertial sensors. Fusing them allows the extraction of instantaneous orientation and acceleration data which in turn enables dead-reckoning. This is a sensor suite with large cumulative error, but with very high bandwidth, suitable for attitude control. In this chapter, we assume that the sensor axes are aligned with the body axes perfectly. A good source of relevant information is [15, p.25].

Accelerometer

An accelerometer installed onboard the aircraft measures the body-frame accelerations **except** the acceleration of gravity. As a result, when the aircraft is laid to rest on the ground the sensor records acceleration with magnitude of 1G, even though the aircraft isn't moving at all. This is similar to the apparent feeling a human has, feeling the force of his weight pulling him down when resting but feeling weightless while in free-fall.

In the ideal case where the accelerometer is installed at the center of gravity of the aircraft, the recorded acceleration is

$$\boldsymbol{a}_{b,m} = \boldsymbol{a}_b - \boldsymbol{R}_b \boldsymbol{g} \tag{5.1}$$

$$= \frac{\boldsymbol{F}_b}{m} - \boldsymbol{R}_b \boldsymbol{g} \tag{5.1a}$$

However, this is an ideal case. Most of the times, the sensor is placed in a point with coordinates $\boldsymbol{r}_{acc}$ relative to the center of gravity. The resulting measurement, affected by the aircraft rotational velocity will be

$$\boldsymbol{a}_{b,m} = \frac{\boldsymbol{F}_b}{m} - \boldsymbol{R}_b \boldsymbol{g} + \dot{\boldsymbol{\omega}}_b \times \boldsymbol{r}_{acc} + \boldsymbol{\omega}_b \times (\boldsymbol{\omega}_b \times \boldsymbol{r}_{acc}) \tag{5.2}$$

which can be expanded into

$$a_{m,x} = \frac{F_x}{m} + g\sin\theta - \dot{r}r_{acc,y} + \dot{q}r_{acc,z} + (-r^2 - q^2)r_{acc,x} + pqr_{acc,y} + prr_{acc,z} \tag{5.2a}$$

$$a_{m,y} = \frac{F_y}{m} - \sin\phi\cos\theta + \dot{r}r_{acc,x} - \dot{p}r_{acc,z} + pqr_{acc,x} + (-p^2 - r^2)r_{acc,y} + qrr_{acc,z} \tag{5.2b}$$

$$a_{m,z} = \frac{F_z}{m} - \cos\phi\cos\theta - \dot{q}r_{acc,x} + \dot{p}r_{acc,y} + prr_{acc,x} + qrr_{acc,y} + (-p^2 - q^2)r_{acc,z} \tag{5.2c}$$

The angular velocity derivatives can be further substituted using eq 2.9.

Gyroscope

Gyroscopes are sensors capable of measuring the rotational velocities of the rigid body they are attached onto. This measurement is unaffected by the location of placement.

$$\boldsymbol{\omega_m} = \boldsymbol{\omega_b} \tag{5.3}$$

Magnetometer

Magnetometers are sensors which measure the magnetic field of the Earth. At any given point on the surface of the Earth the vector field components are known and thus this sensor can be used to extract orientation information. The intensity of the magnetic field (measured usually in nanoTesla) is mostly constant, at about 45 000 nT. However, the direction of the magnetic flux lines changes radically from location to location [16], [17], [8]. If we express the magnetic field intensity as a vector quantity with North, East and Down components, for a given pair of coordinates

$$\boldsymbol{h} = [h_N, h_E, h_D]^T \tag{5.4}$$

then we define as declination the angle

$$dec = \tan^{-1}\left(\frac{h_E}{h_N}\right) \tag{5.5}$$

and the inclination as

$$inc = \tan^{-1} \left(\frac{h_D}{\sqrt{h_N^2 + h_E^2}} \right) \tag{5.6}$$

The measurement of the onboard magnetometer will then be

$$\boldsymbol{h}_m = \boldsymbol{h}_b = \boldsymbol{R}_b \boldsymbol{R}_{inc} \boldsymbol{R}_{dec} \begin{bmatrix} |\boldsymbol{h}| \\ 0 \\ 0 \end{bmatrix} \tag{5.7}$$

AHRS

There also are hardware solutions which incorporate all three aforementioned sensors and extract an estimation of the Euler angles set.

$$\boldsymbol{\Phi}_m = \boldsymbol{\Phi} \tag{5.8}$$

5.2   GPS Measurements

In order to have a reading of the absolute position of the aircraft in the inertial frame, be it the local NED frame or the global frame, defined by latitude and longitude, a GPS sensor is required. This is the only reasonable option, as radio-location is not a viable option for low-cost and low-weight robotic platforms. Whether the system will use a simple GPS receiver, a multi-constellation receiver, differential measurements or even RTK packages improves only the measurement accuracy.

Common quantities reported by a GPS receiver are the longitude, latitude and altitude set. However, these do not correspond to the NED frame. In order to translate them to the north, east and down quantities we need to obtain the data on the curvature of the Earth at the location of interest. The following discussion should be adequate for the needs of a NED frame spanning a few kilometers to each direction of the starting coordinates.

Having done the above necessary conversions, we can treat the GPS receiver as a sensor which reports displacement in the local NED frame

$$\boldsymbol{p}_{gps} = \boldsymbol{p} \tag{5.9}$$

Additionally, most GPS receivers report ground velocities

$$v_{gps} = \|[\dot{n}\ \dot{e}]'\| \tag{5.10}$$

and the direction of travel, also referred to as the *course angle*

$$\chi_{gps} = \text{atan2}\left(\dot{e}, \dot{n}\right) \tag{5.11}$$

5.3 Atmospheric Measurements

Pressure

Having defined the atmospheric model, we can now introduce a barometer sensor, which measures the barometric pressure at the UAV altitude.

$$P_{bar} = P \tag{5.12}$$

Temperature

Also, thermometers are available, which record the atmospheric temperature and are necessary for the extraction of altitude, through pressure readings. Care is needed however, as electronics are known to warm-up and raise the temperature in the enclosed spaces they are placed. However, this discussion belongs to an fault analysis and will not be expanded upon here.

$$T_m = T \tag{5.13}$$

What will be noted here is the fact that thermometers can be used to measure the temperature of components as well, such as batteries, ESCs or motors and provide a health status of those components.

5.4 Air Data

For an efficient and safe aircraft flight, air data measurements are required. These measurements refer to airspeed $\|V_a\|$, angle of attack α and angle of sideslip β.

Airspeed is measured using Pitot tubes, which take into account Bernoulli's equation to convert dynamic air pressure into airspeed readings. Essentially, a barometer is used to perform this reading.

$$P_t = P + \frac{\rho V_a^2}{2} \tag{5.14a}$$
$$P_{t,m} = P_t \tag{5.14b}$$
$$\tag{5.15}$$

Aerodynamic angles α and β can be measured using appropriate instruments, such as wind vanes, but such sensors are seldom found in medium and small UAVs, due to their size and weight.

$$\alpha_m = \alpha \tag{5.16}$$
$$\beta_m = \beta \tag{5.17}$$

5.5   Distance Measurement

Instruments which measure the distance of the UAV from the ground belong to this category. Common types are ultrasonic sensors, laser range finders and LIDARs. Their range varies from a few meters to a few hundred meters and their price range varies accordingly. What all these sensors have in common is that their measurements have a fixed range, varying from $d_{rf,min}$, the minimum reading, up to $d_{rf,max}$, in terms of absolute magnitudes.

$$d_{rf} = \begin{cases} d_{rf,min} & , d > d_{rf,min} \\ d & , h \in [d_{rf,min}, d_{rf,max}] \\ d_{rm,max} & , d < d_{rf,max} \end{cases} \tag{5.18}$$

Some confusion may be caused by the direction of the comparison ranges, but keep in mind that using the NED frame, d is negative when the airplane is above ground altitude.

5.6   Voltage Measurement

Voltage Measurement is a very useful means to assess the remaining energy capacity of an onboard battery. Even though the relation between remaining energy and output voltage is not linear, useful conclusions can be extracted.

In general, any voltage level can be measured by such an instrument

$$V_{i,m} = V_i \tag{5.19}$$

but in the specific case of the battery voltage measurement we have

$$V_{B,m} = V_B - I_o R_B \tag{5.20}$$

5.7   Current Measurement

Similarly to voltage measurements, current measurements are available as well. These are useful to monitor the power consumption of the aircraft and, in extension, are a valid means to approach the thrust produced by the power plant.

Usually, current sensors are placed on the battery leads, since their most common occurrence measures only DC current.

$$I_{o,m} = I_o \tag{5.21}$$

5.8　Motor Angular Velocity Measurement

Finally, a quantity with great informational content is the rotational velocity of the motor shaft. This can be measured with commercial RPM sensors and can provide information on the thrust produced or even the health status of the motor itself.

$$n_m = n \tag{5.22}$$

Bibliography

[1] US Standard Atmosphere, 1976. Technical report, National Oceanic and Atmospheric Administration, National Aeronautics and Space Adminisration, United States Air Force, 1976.

[2] D Allerton. *Principles of flight simulation*. Wiley, 2009.

[3] Francisco Bañuelos Ruedas, César Angeles-Camacho, and Sebastián Rios-Marcuello. Methodologies Used in the Extrapolation of Wind Speed Data at Different Heights and Its Impact in the Wind Energy Resource Assessment in a Region. In Gastn Orlando Suvire, editor, *Wind Farm - Technical Regulations, Potential Estimation and Siting Assessment*, chapter 4. InTech, June 2011.

[4] T. R. Beal. Digital simulation of atmospheric turbulence for Dryden and von Karman models. *Journal of Guidance, Control, and Dynamics*, 16(1):132–138, January 1993.

[5] RW Beard and TW McLain. *Small unmanned aircraft: Theory and practice*. 2012.

[6] Paul Berner and D Ph. Orientation, Rotation, Velocity, and Acceleration and the SRM. Technical Report June, 2008.

[7] John Carri. A four-constant model for electric motors (Draft No. 2). Technical Report 2, 2007.

[8] NOAA National Geophysical Data Center. Geomagnetism. `http://www.ngdc.noaa.gov/geomag/geomag.shtml`. [Online; accessed 13-January-2015].

[9] V Klein and EA Morelli. *Aircraft system identification: theory and practice*. AIAA, 2006.

[10] Jack W. Langelaan, Nicholas Alley, and James Neidhoefer. Wind Field Estimation for Small Unmanned Aerial Vehicles. *Journal of Guidance, Control, and Dynamics*, 34(4):1016–1030, July 2011.

[11] MathWorks. Aerospace toolbox documentation: Dryden wind turbulence model (continuous). `http://www.mathworks.com/help/aeroblks/`

`drydenwindturbulencemodelcontinuous.html`, 2015. [Online; accessed 8-January-2015].

[12] David J. Moorhouse and Robert J. Woodcock. Background Information and User Guide for MIL-F-8785C, Military Specification - Flying Qualities of Piloted Airplanes. Technical report, Air Force Wright Aeronautical Laboratories, 1982.

[13] WM Mulaire. Department of Defense: World Geodetic System 1984. Technical report, National Imagery and Mapping Agency, 2000.

[14] EW Peterson and JP Hennessey Jr. On the use of power laws for estimates of wind power potential. *Journal of Applied Meteorology*, 1978.

[15] BL Stevens and FL Lewis. *Aircraft control and simulation.* John Wiley & Sons, illustrate edition.

[16] Wikipedia. Magnetic declination. `https://en.wikipedia.org/wiki/Magnetic_declination`, 2015. [Online; accessed 13-January-2015].

[17] Wikipedia. Magnetic dip. `https://en.wikipedia.org/wiki/Magnetic_dip`, 2015. [Online; accessed 13-January-2015].

[18] Wikipedia. Wind gradient. `http://en.wikipedia.org/wiki/Wind_gradient`, 2015. [Online; accessed 8-January-2015].

[19] Wikipedia. Wind profile power law. `http://en.wikipedia.org/wiki/Wind_profile_power_law`, 2015. [Online; accessed 8-January-2015].